

Sr-DOPING EFFECT ON APATITE TYPE $\text{La}_{10}\text{Si}_6\text{O}_{27}$ ELECTROLYTE: EXPERIMENTS AND AB-INITIO CALCULATION

Yangzhou Ma^{1, 2, 3*}, Nouredine Fenineche^{1, 3}, Omar Elkedim^{2, 3}, Michel Moliere¹

¹ School of Materials Science and Engineering, Anhui University of Technology, Ma'anshan, 243002, PR China

² ICB UMR 6303, CNRS, Université de Bourgogne Franche-Comté, UTBM, F-90010, Belfort, France

³ FEMTO-ST, UBFC, UTBM, Site de Sévenans, 90010, Belfort Cedex, France

*e-mail: yangzhou.ma@outlook.com

Abstract. Apatite-type lanthanum silicates draw researchers' attention due to their good performance as electrolyte materials for IT-SOFC (intermediate temperature solid oxide fuel cells). In this paper we present Sr-doping effect on $\text{La}_{10}\text{Si}_6\text{O}_{27}$ (LSO) via experimental method and ab-initio calculation: the samples were prepared through an optimized water-based sol-gel process. High purity, crystallinity compounds with and without Sr-doping LSO are obtained and the resulting materials were characterized by scanning electron microscopy, X-ray diffraction and energy-dispersive X-ray spectroscopy. Ionic conductivities and activation energies have been measured after sintering at 1500 °C and the effect of the Sr-doping has been investigated. The results show that the ionic conductivity is thermally activated and values lies between 4.5×10^{-2} and $1 \times 10^{-6} \text{ Scm}^{-1}$ at 873 K as a function of the Sr-doping ratio. The ab-initio calculation work shows the lattice parameter and band structure affected by Sr-doping, leading to the change of macro scope properties. The calculation results of activation energies were consistent with those obtained by experiments.

1. Introduction

With various advantages to directly and efficiently convert chemical energy to electrical energy, fuel cells have been investigated and applied in many fields [1-3]. Among them, solid oxide fuel cells (SOFCs) draw much attention in a commercial application with a solid material as the electrolyte [4,5]. The electrolyte has excellent ionic conductivity negligible electronic conduction over a wide range of oxygen partial pressure. Nevertheless, the traditional SOFC has too high operating temperature (800 °C – 1000 °C). The high temperature causes many problems, such as the ageing of constituent components, the choice of the matched interconnectors or electrodes [6], and the maintenance of high temperature itself will cost much, which would restrict the application in many fields. Recently, some new solid electrolyte materials have been developed to overcome these problems. These materials have common features: high ionic conductivity and intermediate operating temperature. Among these, apatitetype lanthanum silicate, with a common formula $\text{La}_{10}\text{Si}_6\text{O}_{27}$, has been considered as a promising solid electrolyte for intermediate temperature SOFC (IT-SOFC) since it was firstly reported to have higher conductivity than YSZ (Yttria-stabilized zirconia) below 600 °C by S. Nakayama et al [7,8]. This series material has significant characteristics of friendly operating temperature and high oxygen ion transportation efficiency under various oxygen partial pressures [9]. Multiple doping elements were also employed in the compound to improve the apatite $\text{La}_{10}\text{Si}_6\text{O}_{27}$ performance as an electrolyte. Because of the similar chemical properties with La, Sr has been chosen as suitable element doping at La site. Recently, Sr-doped

LSO $\text{La}_9\text{Sr}_1\text{Si}_6\text{O}_{26.5}$ has been synthesized by Bonhomme et al with solid state reaction [10] and the ionic conductivity is 2.4 to 2.6 $\text{mS}\cdot\text{cm}^{-1}$ at 700 °C. As for the influence of different doping ratios, A. Orera et al. [11] has investigated the ionic conductivity of $\text{La}_{8+x}\text{Sr}_{2-x}(\text{SiO}_4)_6\text{O}_{2+0.5x}$ ($0 \leq x \leq 1.0$) with ^{29}Si NMR and Raman technologies. The solid state reaction is used to synthesize the apatite, however, there are still a small amount of La_2SiO_5 impurities was observed even with high sintering temperature.

Ab-initio calculation methods was also widely used to analyze the material microstructure, properties and performances. As one of these methods, density functional theory (DFT) is normally regarded as a more efficient and economical way to get crystal parameters, electronic structures, formation energy, and magnetic properties [12,17]. Meanwhile, the oxygen diffusion in different types of electrolyte including LSO electrolyte has been summarized by Chroneos et al. [18], and the ionic transportation mechanism has been studied using atomistic simulation. However, only few studies focusing on the apatite electrolyte for SOFC using DFT are available.

In this study, on one hand, a simple water-based sol-gel [19,20] method has been adopted to obtain LSO and Sr-doped LSO. We have obtained pure apatite composition with and without Sr-doping under moderate calcination temperature. The influence to the ionic conductivity also has been investigated with different doping ratios. On the other hand, based on DFT, systematic computational results of Sr-doped LSO apatite for SOFC electrolyte are presented and doping position effect on the ionic conductivity and activation energy are also studied. Calculation results are also compared to previous experimental results.

2. Experimental and calculation details

The $\text{La}_{10-x}\text{Sr}_x\text{Si}_6\text{O}_{27-0.5x}$ ($x=0, 1, 2$) powders are synthesized by a water-based sol-gel technique using $\text{La}(\text{NO}_3)_3\cdot 6\text{H}_2\text{O}$, $\text{Sr}(\text{NO}_3)_2$ and TEOS (tetraethyl orthosilicate) (all from sigma-Aldrich, 99.9%) as raw materials. Procedure involved in the synthesis of the apatite LSO powders are showed in Fig. 1. The obtained groups of sol are treated in a drying oven to get the dry gel. They are compressed with 200Mpa for 30s, and then, calcined in air at 900°C with a heating rate of 10°C/min and then free cooled. The following sintering process are employed to density the samples with the temperature of 1500°C for 2h. The crystalline phase are identified by X-ray diffraction (XRD) analysis (Bruker AXS D8 Focus) using the Cu $\text{K}\alpha$ radiation ($\lambda=1.5406 \text{ \AA}$). The microstructure characterization of the obtained powders is performed by a JSM5800LV (JEOL, Japan) scanning electron microscopy (SEM) combined with EDX support.

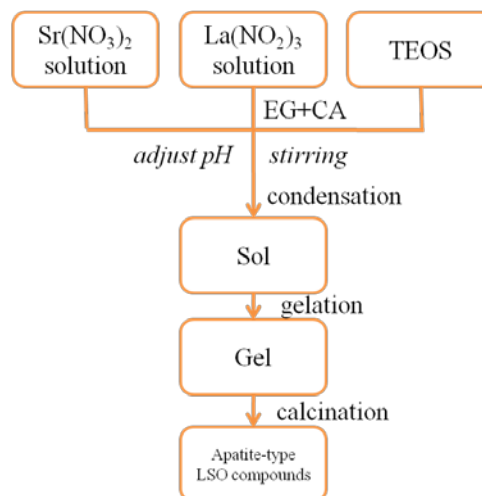


Fig. 1. Flow chart of the process used in the preparation of lanthanum silicate apatites.

Ultrasoft pseudo potential [21] method based on density functional theory (DFT) in the generalized gradient approximation (GGA) proposed by Perdew et al. [22] was used to perform the calculations. The Vienna ab initio simulation package (VASP) [23-25] was used to explore the influence of doping positions by applying a plane-wave basis within the projector augmented-wave method. As a first step, a single apatite cell was built to obtain the DOS calculation results through the structure optimization and static calculation. The Brillouin zone scale was set to $3 \times 3 \times 3$ gamma centered k-point mesh in the Monkhorst–Pack scheme [26]. Nevertheless, the k-point was changed to $7 \times 7 \times 7$ in the DOS calculation. An energy cut-off of 380 eV was used in all of our calculations.

3. Results and discussions

Fig. 2 shows the apatite structure of $\text{La}_{10}\text{Si}_6\text{O}_{27}$ which belongs to the $p6_3/m$ group of the hexagonal lattice systems. The crystals are hexagonal with corner angles of 120° and 60° . The major oxygen ions migration channel lies at the interstitial O position. There are two types of Lanthanum sites: $6h$ - near to the major channel and $4f$ - far from the major channel. Sr atoms substitute or partial substitute at La sites.

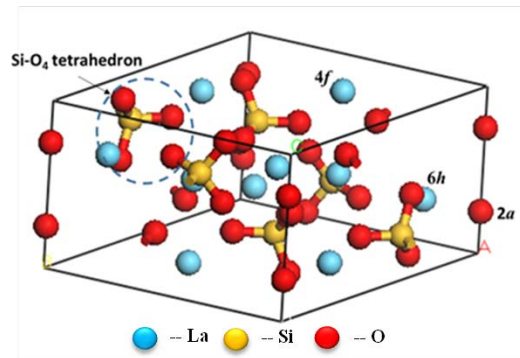


Fig. 2. Sketch of the LSO apatite structure.

In order to verify the purity of the compounds and investigate the lattice constant change with Sr-doping, Fig. 3 gives the diffraction patterns of the compounds with different Sr-doping ratios. All the major diffraction peaks are inferred to apatite phase. The intensity has scarcely changed among these three groups which means the compounds (with and without Sr-doping) have well crystallized.

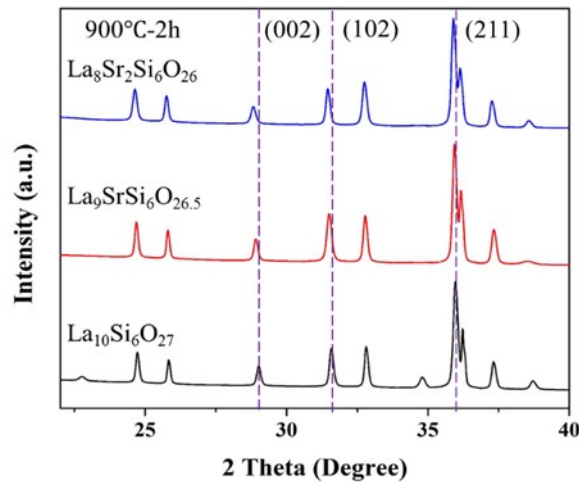


Fig. 3. XRD patterns of the products with different and Sr-doping ratios.

By seeing the peaks of various mille index, we find a relatively obvious shift to low angle with the increase of Sr proportion. This phenomenon is more evident along c-axis [mille index (002)]. Thus the lattice constant enlarges, particularly along c-axis, with Sr-doping ratios increasing. This will affect the oxygen ion migration channel, then to the performance as electrolyte in SOFC.

This change of the lattice constant is summarized in Table 1, as well as the calculation results. Sr-doping has a major effect on the lattice parameter of c-axis, instead of that of a, b-axis. It can be seen the calculation work gives precise prediction of the lattice constant. Meanwhile, the electronic properties of the material can be calculated with this crystal model.

Table 1. Calculated and experimental LSOs lattice constants.

	Experiment		Calculation	
	a/Å	c/Å	a/Å	c/Å
(La ₁₀ Sr ₀)Si ₆ O ₂₇	9.72	7.19	9.6759	7.1889
(La ₉ Sr ₁)Si ₆ O _{26.5}	9.71	7.20	9.6924	7.1918
(La ₈ Sr ₂)Si ₆ O ₂₆	9.71	7.24	9.6760	7.2341

The morphologies of the samples have been characterized and Fig.4 illustrates the morphology of the obtained sample by the SEM micrograph. The grains are close packed with each other which is suitable to prevent the gas exchange during the fuel cell operation process. The size is about 23μm which means the sample is well crystallized. Notably, the hexagonal crystal structure prefers to form the grain with hexagonal shape which has a high abundance in our samples. It can be said in one respect that the apatite phase lanthanum silicates with and without Sr-doping have been obtained by the water-based sol-gel method.

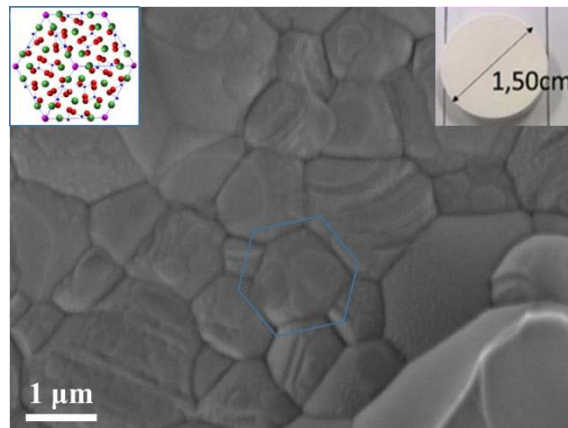


Fig. 4. The SEM micrograph showing the morphology of the obtained sample by (the top left inset shows the crystal structure of apatite type LSO; the top right inset shows the shape of the sample).

Fig.5 shows the ionic conductivity results of the samples with different Sr-doping ratios. Sr-doping affects the ionic conductivity significantly. The best conductivity at intermediate temperature is the undoped La₁₀Si₆O₂₇ apatite having a very high conductivity (45 mS•cm⁻¹) at 800°C. Note worthily the La₉SrSi₆O_{26.5} apatite also has a considerable conductivity (38.3 mS•cm⁻¹ at 600°C) being significantly higher than the general conductivity levels reported in previous works using traditional synthesis methods. This “medium Sr-doped” LSO is therefore suitable for low temperature SOFC applications. High ratio of Sr-doping leads to mediocre ionic conductivity.

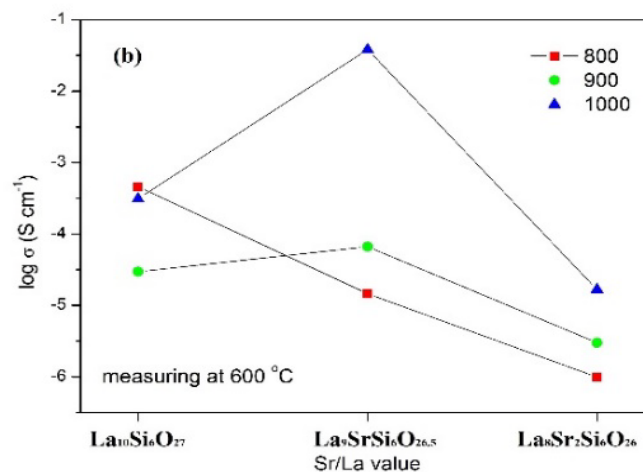


Fig. 5. Arrhenius plots of samples with different Sr doping ratios.

In order to evaluate the activation energy of the compounds with different Sr-doping ratio, Fig. 6 shows the energy barrier of oxygen migration by the calculation work. A model of oxygen migration along the major ionic channel. For the considered doping effect, the migration channel can be supposed directly along c-axis. The energy barrier is approximated as the activation energy.

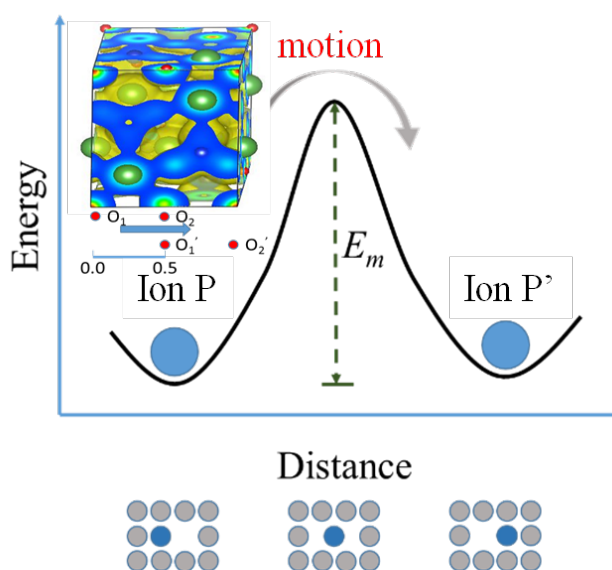


Fig.6. The calculated energy barriers along c-axis for activation energy of LSO.

Fig. 7 gives the comparison chart of activation energies with different Sr-doping ratios. Sr-doping effect on the activation energy seems to be significant. Indeed, more Sr-doping ratio leads to higher activation energy, which is not suitable for electrolyte performances in SOFC. This phenomenon is also consistent with the experimental results: too high Sr-doping ratio results in high activation energy. Meanwhile, one Sr-doping slightly affects the activation energy in experimental results which because of the experimental process has an influence on the activation energy.

It also can be noted that the doping effect is more significant for the substitution at La 6h position (near the migration channel) than that at La 4f position (far from the migration channel). The Sr-doping actually affects the migration channel and the results depend on the distance to the channel. The calculated activation energy is higher than the experimental one

may be ascribable to the actual migration channel being not along a straight line. Even so the tendency to influence the activation energy is obvious in both the experiments and calculation with the Sr-doping: too high Sr-doping ratio leads the sample to have low ionic conductivity and high activation energy.

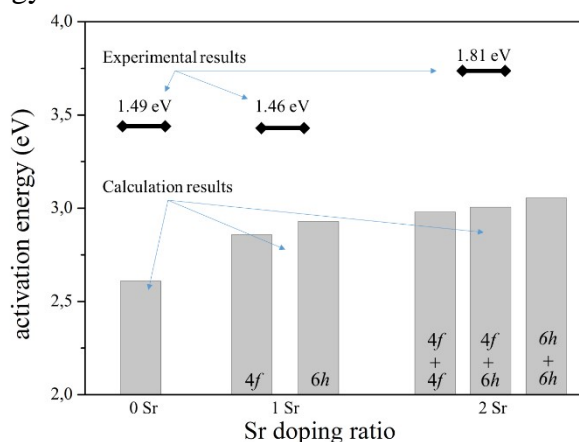


Fig. 7. The calculated energy barriers along c-axis for the activation energy of each group.

4. Conclusions

Lanthanum silicate oxides have been synthesized with and without Sr-doping for potential applications as oxygen ion conducting electrolytes in IT-SOFCs. The compounds obtained are pure, well crystallized apatites and that Sr is well incorporated in the structure. The effects of Sr-doping ratios have been investigated by both experimental and calculation ways. The non-doped $\text{La}_{10}\text{Si}_6\text{O}_{27}$ exhibited an ionic conductivity of $45 \text{ mS}\cdot\text{cm}^{-1}$ at 800°C . Meanwhile a remarkable, intermediate temperature conductivity of $38.3 \text{ mS}\cdot\text{cm}^{-1}$ is obtained at 600°C with the $\text{La}_9\text{SrSi}_6\text{O}_{26.5}$ formula. The $\text{La}_8\text{Sr}_2\text{Si}_6\text{O}_{26}$ gives a lower conductivity and higher activation energy than those of low doping groups. The phenomena are caused by the alteration of the lattice parameters and ion migration barrier energy, which is demonstrated by the calculation work.

Acknowledgments. The authors gratefully acknowledge financial support from China Scholarship Council (CSC) and the Mésocentre de calcul de Franche-Comté for providing the calculation software. In addition, we would like to show our gratitude to Mr. P. Briois for the electrical properties measurement.

References

- [1] H. Jung, S.-H. Choi, H. Kim, J.-W. Son, J. Kim, H.-W. Lee, J.-H. Lee // *Journal of power sources* **159** (2006) 478.
- [2] C. Bernay, M. Marchand, M. Cassir // *Journal of Power Sources* **108** (2002) 139.
- [3] S. Park, J.M. Vohs, R.J. Gorte // *Nature* **404** (2000) 265.
- [4] S. Chen, Y. Chen, H. Finklea, X. Song, G. Hackett, K. Gerdes // *Solid State Ionics* **206** (2012) 104.
- [5] R. Fernández-González, T. Molina, S. Savvin, R. Moreno, A. Makradi, P. Núñez // *Ceramics International* **40** (2014) 14253.
- [6] J.B. Goodenough // *Annual review of materials research* **33** (2003) 91.
- [7] S. Nakayama, T. Kageyama, H. Aono, Y. Sadaoka // *Journal of Materials Chemistry* **5** (1995) 1801.
- [8] T. Mimani, K. Patil // *Materials Physics and Mechanics* **4** (2001) 134.

- [9] Y. Pivak, V. Kharton, A. Yaremchenko, S. Yakovlev, A. Kovalevsky, J. Frade, F. Marques // *Journal of the European Ceramic Society* **27** (2007) 2445.
- [10] C. Bonhomme, S. Beaudet-Savignat, T. Chartier, P.-M. Geffroy, A.-L. Sauvet // *Journal of the European Ceramic Society* **29** (2009) 1781.
- [11] A. Orera, E. Kendrick, D. Apperley, V. Orera, P. Slater // *Dalton Transactions* (2008) 5296.
- [12] S. Lardjane, G. Merad, N. Fenineche, A. Billard, H. Faraoun // *Journal of Alloys and Compounds* **551** (2013) 306.
- [13] Y. Bouhadda, M. Bououdina, N. Fenineche, Y. Boudouma // *Computational Materials Science* **78** (2013) 110.
- [14] Y. Xu, Z. Zhang, S. Mao, Y. Ma // *Applied Surface Science* **280** (2013) 247.
- [15] O. Kozlova, M. Zelenina // *Materials Physics and Mechanics* **20** (2014) 51.
- [16] A. Sliogeris, J. Tamuliene, R. Vaisnoras // *Materials Physics and Mechanics* **12** (2011) 186.
- [17] V.V. Nelayev, A.I. Mironchik // *Materials Physics and Mechanics* **9** (2010) 26.
- [18] A. Chroneos, B. Yildiz, A. Tarancón, D. Parfitt, J.A. Kilner // *Energy & Environmental Science* **4** (2011) 2774.
- [19] V. Kondratiev, I. Kink, A. Romanov // *Materials Physics and Mechanics* **17** (2013) 38.
- [20] S. Tao, J.T. Irvine // *Materials research bulletin* **36** (2001) 1245.
- [21] D. Vanderbilt // *Physical Review B* **41** (1990) 7892.
- [22] J.P. Perdew, J. Chevary, S. Vosko, K.A. Jackson, M.R. Pederson, D. Singh, C. Fiolhais // *Physical Review B* **46** (1992) 6671.
- [23] G. Kresse, D. Joubert // *Physical Review B* **59** (1999) 1758.
- [24] G. Kresse, J. Furthmüller // *Computational Materials Science* **6** (1996) 15.
- [25] G. Kresse, J. Furthmüller // *Physical Review B* **54** (1996) 11169.
- [26] H.J. Monkhorst, J.D. Pack // *Physical Review B* **13** (1976) 5188.